Energy & Environmental Science

Cite this: *Energy Environ. Sci.*, 2012, **5**, 6953

www.rsc.org/ees

PAPER

Improving the light-harvesting of amorphous silicon solar cells with photochemical upconversion

Yuen Yap Cheng,†[a] Burkhard Fückel,†[a] Rowan W. MacQueen,[a] Tony Khoury,[a] Raphaël G. C. R. Clady,[a] Tim F. Schulze,[a] N. J. Ekins-Daukes,[b] Maxwell J. Crossley,[a] Bernd Stannowski,[c] Klaus Lips‡[d] and Timothy W. Schmidt§[ae]

Received 17th January 2012, Accepted 9th February 2012
DOI: 10.1039/c2ee21136j

Single-threshold solar cells are fundamentally limited by their ability to harvest only those photons above a certain energy. Harvesting below-threshold photons and re-radiating this energy at a shorter wavelength would thus boost the efficiency of such devices. We report an increase in light harvesting efficiency of a hydrogenated amorphous silicon (a-Si:H) thin-film solar cell due to a rear upconvertor based on sensitized triplet–triplet-annihilation in organic molecules. Low energy light in the range 600–750 nm is converted to 550–600 nm light due to the incoherent photochemical process. A peak efficiency enhancement of (1.0 ± 0.2)% at 720 nm is measured under irradiation equivalent to (48 ± 3) suns (AM1.5). We discuss the pathways to be explored in adapting photochemical UC for application in various single threshold devices.

Introduction

Photovoltaics (PV) offer a solution for the development of sustainable energy sources, relying on the sheer abundance of sunlight: More sunlight falls on the Earth's surface in one hour than is required by its inhabitants in a year. However, it is imperative to manage the wide distribution of photon energies available in order to generate more cost efficient PV devices because single threshold PV devices are fundamentally limited to a maximum conversion efficiency, the Shockley-Queisser (SQ) limit.[1] Recent progress has enabled the production of c-Si cells with efficiencies as high as 25%,[2] close to the limiting efficiency of ~30%. But these cells are rather expensive, and ultimately the cost of energy is determined by the ratio of material cost to the efficiency of the PV device. A strategy to radically decrease this ratio is to circumvent the SQ limit in cheaper, second generation PV devices. This is the goal of third-generation photovoltaics.[3]

One promising approach is the use of hydrogenated amorphous silicon (a-Si:H), where film thicknesses on the order of several 100 nm are sufficient, hence reducing the material cost significantly. Unfortunately, the optical threshold of a-Si:H is rather high (1.7–1.8 eV) and the material suffers from light-induced degradation.[4] Thinner absorber layers in a-Si:H devices are generally more stable than thicker films due to the better charge carrier extraction, but at the expense of reduced conversion efficiencies, especially in the red part of the solar spectrum

[a]*School of Chemistry, The University of Sydney, NSW 2006, Australia*
[b]*Department of Physics and the Grantham Institute for Climate Change, Imperial College, London, UK SW7 2AZ*
[c]*Competence Centre Thin-Film- and Nanotechnology for Photovoltaics Berlin (PVcomB), Helmholtz-Zentrum Berlin für Materialien und Energie, 12489 Berlin, Germany*
[d]*Institute for Silicon Photovoltaics, Helmholtz-Zentrum Berlin für Materialien und Energie, 12489 Berlin, Germany*
[e]*Institute of Photonics and Optical Science, The University of Sydney, NSW 2006, Australia*
† These authors contributed equally to this study.
‡ lips@helmholtz-berlin.de
§ t.schmidt@chem.usyd.edu.au

Broader context

Solar energy devices with a single energy threshold suffer from an inability to harvest more than about 30% of the energy available from the sun (unconcentrated). This limit, first derived by Shockley and Queisser, is due, in part, to the inability to harvest photons with energies below the threshold. A way to address this loss is by manipulating the solar spectrum with upconversion (joining two low energy photons together) to increase the solar cell efficiency. Recent progress has been made in the field of photochemical upconversion which has the potential to operate under unconcentrated sunlight in the future. In this article, we apply photochemical upconversion to amorphous silicon solar cells, demonstrating proof-of-principle and outlining the pathway required to move this technology towards practical application.

where the absorption coefficient is diminished. Indeed, for all higher bandgap materials, which includes a-Si:H as well as organic and dye-sensitized cells, the major loss mechanism is the inability to harvest low energy photons.[5,6]

Ways to overcome the single threshold paradigm by harvesting low energy photons are realised in tandem and multijunction devices and proposed in intermediate-band solar cells.[7,8] However, these approaches require reengineering of the solar cell architecture, which comes at increased cost. A method to improve existing solar cell technology is upconversion (UC) of low energy photons. Here, a UC unit is placed behind a bifacial solar cell (SC) such that the low energy photons transmitted by the SC are converted into photons above the bandgap and radiated back into the SC.[9] For UC to operate under incoherent sunlight conditions – in contrast to second harmonic generation, for instance, – an intermediate energy level must be available, preferably long-lived. As pointed out by Trupke *et al.*,[10] the UC efficiency increases if the intermediate level has a substructure such that the initially populated state can relax into a lower-lying state which is not radiatively coupled to the ground state, thereby temporarily storing energy.

In photochemical UC effected with dye-sensitised triplet–triplet annihilation (TTA), this is the case.[11] As depicted in Fig. 1 (a), sensitizer molecules are promoted from the S_0 singlet ground state to S_1 by absorbing low energy photons ($h\nu_1$). Intersystem crossing results in a non-adiabatic transition to the long-lived T_1 triplet state, satisfying the aforementioned energy sacrifice requirements. Subsequent triplet energy transfer (TET) to emitter molecules (in excess) produces a population of emitter triplets which then undergo triplet–triplet annihilation (TTA) to produce $S_1 \rightarrow S_0$ emission at a higher energy than the photons absorbed ($h\nu_2$). In recent years, a number of different sensitizer-emitter combinations have been reported as potent TTA-UC systems[12,13] with recent applications in displays[14] and biological imaging.[15]

In this contribution, we report the first integrated a-Si:H/TTA-UC photovoltaic device, as a proof-of-principle of a third generation device. We demonstrate how to characterize such a UC-SC system so that its performance under solar conditions may be evaluated. Furthermore, we outline the path needed to improve the device so that it will operate efficiently under unconcentrated solar conditions.

Experimental

UC materials

The dyes utilized in these investigations are: Two palladium porphyrins, PQ_4Pd and PQ_4PdNA, as light-harvesting (sensitizer) materials; and rubrene as the emitting species (Fig. 1 (b)), dissolved in toluene. Rubrene (Sigma-Aldrich) was used as purchased and the tetrakisquinoxalinoporphyrin PQ_4Pd was synthesized as reported.[16] Similarly, the derivative PQ_4PdNA was prepared. Its detailed synthesis and characterisation is to be reported elsewhere. The compounds were dissolved in toluene (PQ_4Pd 3.3×10^{-4} M, rubrene 5.1×10^{-3} M and PQ_4PdNA 1.5×10^{-4} M, rubrene 2.7×10^{-3} M) and the solutions were transferred in custom made vacuum cuvettes (1 cm pathlength) and degassed by at least 3 freeze-pump-thaw cycles ($\sim 10^{-6}$ mbar), to prevent quenching of the triplet states by molecular oxygen. One side of the UC cuvette was optically coupled to the backside of the SC with a thin film of immersion oil (Sigma-Aldrich, $n_D^{20} = 1.516$).

The photophysics of the PQ_4Pd-based UC system are fully characterized: Previously, it was found to have a limiting UC efficiency $\eta_{UC,max} = 30\%$ based on the TTA process,[17,18] without taking reabsorption into account. η_{UC} is the ratio of upconverted photons to incoming photons; *i.e.* an ideal UC system can proceed with $\eta_{UC} = 50\%$ at most. The slightly modified sensitizer PQ_4PdNA was recently synthesized and is explored due to its advantageous red-shifted and increased (integrated) absorbance (Fig. 2 (b)).

Integrated SC/UC device

Thin bifacial a-Si:H *p-i-n* solar cells were grown in an plasma-enhanced chemical vapor deposition (PECVD) cluster tool (AKT1600A) at 200 °C on commercial, natively-textured 30 cm × 30 cm transparent conducting oxide (TCO: SnO_2:F) glass substrates at the PVcomB at Helmholtz-Zentrum Berlin für Materialien und Energie (HZB). A 300 nm film of sputtered ZnO:Al was used as back contact to form bifacial SCs. The highly doped *p* -a-SiC:H and *n* -a-Si:H layers were 10 and 20 nm thick, respectively. To match the absorption profile of the respective UC unit as depicted in Fig. 3, we reduced the *i* -layer thickness of the *p-i-n* cells to 50 nm or 100 nm, and forewent the

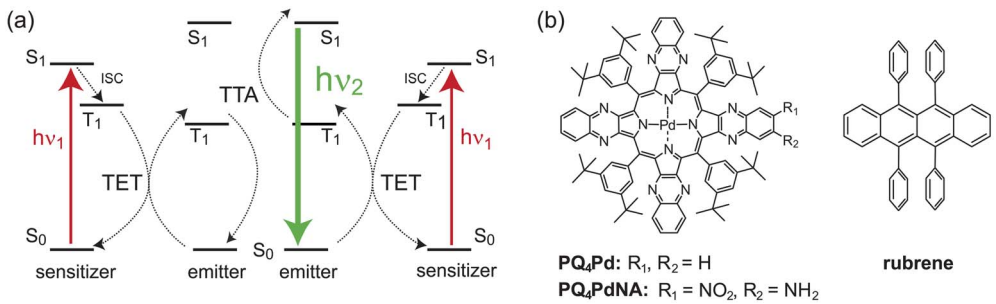

Fig. 1 (a) Scheme for dye sensitized triplet–triplet annihilation (TTA) depicting the molecular states involved. After photoexcitation with low energy light ($h\nu_1$), the sensitizer undergoes efficient intersystem crossing (ISC) to its triplet state T_1. Subsequent triplet energy transfer (TET) to the emitter manifold leads to triplet–triplet annihilation (TTA) of two emitter T_1 states to bring about upconverted fluorescence ($h\nu_2$). (b) The molecules utilized for photochemical upconversion: Two Pd porphyrins, PQ_4Pd and PQ_4PdNA, were employed as sensitizers in combination with the highly efficient TTA emitter rubrene.

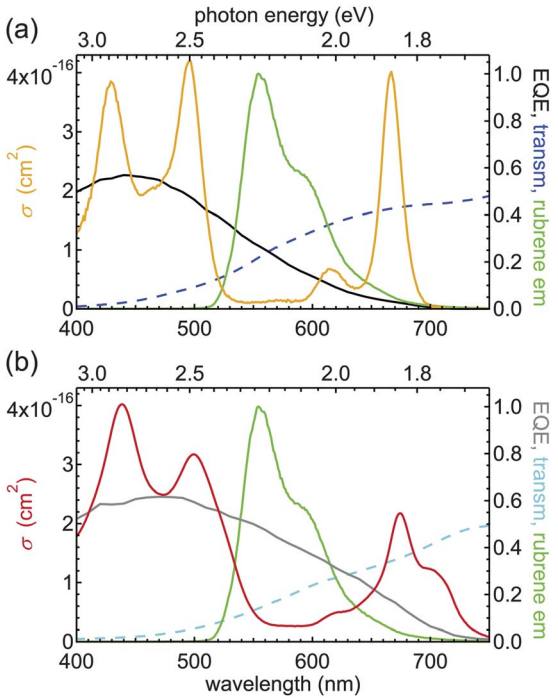

Fig. 2 Spectral characterisation: Comparison of the EQE (black for 50 nm, grey for 100 nm *i* -layer) and transmission curves (dashed) of the respective a-Si:H solar cell with the absorption cross section (σ, orange or red) and emission (green) profile of the UC unit constituents. (a) 50 nm a-Si:H solar cell and PQ_4Pd, (b) 100 nm a-Si:H solar cell and PQ_4PdNA.

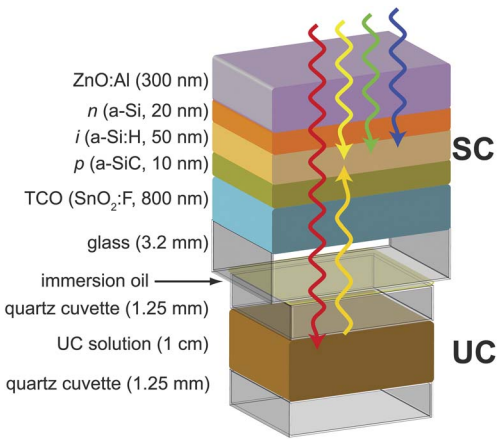

Fig. 3 A cartoon of the integrated a-Si:H *p-i-n*/UC device. Low energy (shown in red) photons pass though the *p-i-n* structure and excite dye molecules in the upconversion unit, which subsequently returns photons of a shorter wavelength (yellow).

implementation of light trapping schemes. For the special requirement of the experimental setup, the superstrate SC was illuminated through the transparent ZnO:Al back contact. Considering this and the ultra thin *i* -layer, the AM1.5G efficiency of both SCs amounts to (2 ± 0.2%).

The SCs of both devices show hardly any light-induced degradation and their optical transparencies match the conversion profiles of the respective UC units. The UC unit is placed behind the bifacial a-Si:H SC so that low energy light (below the bandgap) can pass through the SC and reach the UC unit with the upconverted light fluorescing back onto the SC.

Determination of SC enhancement through UC

An EQE measurement determines the linear current response of the SC to a photon flux. However, to evaluate the effect of the UC unit on the EQE of the SC, it must be taken into account that photochemical UC is a non-linear process at low excitation densities. Indeed, for every TTA-UC system, the dependence of the UC photon fluence on the continuous irradiance becomes linear only above a certain power threshold due to the competition between first and second order triplet decay in the emitter manifold.[19,20] A measurement under a weak monochromated beam alone would neglect the excitation of the UC unit by other wavelengths under broadband solar illumination. To measure the EQE curve of the a-Si:H *p-i-n*/UC device with the UC under controlled operating conditions, one should measure the linear response at a given triplet concentration in the UC material which is then mapped onto a solar concentration factor.

The light sources used in our setup, Fig. 4, are a broadband, ozone free, 1 kW Xe long arc lamp (Oriel) as probe and a 1.2 mW 670 nm cw laser diode (Lastek) as pump. Upon failure, the probe light source was replaced by a 150 W halogen lamp (Philips 7158) which resulted in a weaker probe with increased noise (PQ_4PdNA). The broadband light of the probe is chopped and passed through a computer-driven monochromator stage (Spectral Products CM110, 14 nm bandpass) to scan the irradiation wavelength before reaching the device. Typical intensities of the probe light at one wavelength were in the range of 0.6 mW cm^{-2} (halogen lamp) and 8 mW cm^{-2} (Xe arc lamp). A 405 nm long pass filter (BLP01-405*R*-25) after the probe source prevented second-order diffracted light from reaching the SC. The probe light was split with a glass slide (4% reflectivity) and its intensity was monitored by a power meter (Newport 1936-C) with a wavelength-calibrated silicon photodiode (918 D-UV-OD3) simultaneously to the measurements. An optical chopper (Thorlabs) modulated the probe light with a reference frequency (~100 Hz) used for lock-in detection. The beams were

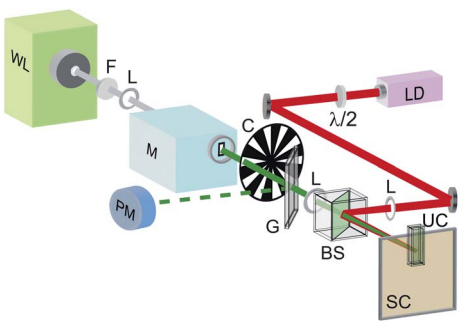

Fig. 4 Setup for the measurement of the enhancement of solar cells (SC) by an upconvertor (UC). The sample SC and UC are irradiated by the chopped (C) white light (WL) probe beam passed through a 405 nm longpass filter (F) and a monochromator (M). The probe beam is split with a glass slide (G) and the reflection is monitored by a power meter (PM). The current of the solar cell is measured by lock-in amplification. A background concentration of triplet molecules for the photochemical upconversion is generated by (unchopped) light of a 670 nm cw laser diode (LD) superposed with the probe light beam by a polarising beam splitter (BS). The pump polarization is adjusted by a λ/2 wave plate. The beams are focussed through the SC onto the UC by lenses (L).

superposed and guided through the SC into the UC solution with a polarising beam splitter and the irradiation of the laser diode could be adjusted with a half-wave plate (Thorlabs).

The SC short circuit current due to the chopped probe light was preamplified (Stanford Research SR570) and fed into a dynamic signal acquisition device (National Instruments USB-4431) and analysed with in-house LabVIEW software. The homogeneity of the laser diode was ensured using a Coherent beam profiler in far field and at the upconversion unit.

The 670 nm laser generates a background triplet concentration that can be translated into equivalents of solar irradiation (in units of the AM1.5 spectrum of the sun, ⊙). The current generated by the SC is pre-amplified and monitored by a lock-in amplifier, suppressing the background current created by the laser diode beam (and other potential sources). Compared to the chopper frequency (~100 Hz), the build-up and decay of steady-state conditions in the UC unit (~100 μs)[17,18] are negligible.

The setup, as described, allows measurement of the wavelength-dependent response of the SC in terms of the generated current. To determine the effect of UC, different measurements are conceivable, *e.g.* comparison of the response curve with and without the UC unit. However, this naïve approach would not take into account first order effects such as reflection, and fluorescence from the directly excited emitter, hence leading to a contorted result. In principle, these problems can be solved by comparing a working, degassed UC with a non-working, aerated UC unit. But, the singlet oxygen produced in the reference measurement leads to fast photodegradation of rubrene, altering the properties of the aerated UC unit. Furthermore, the local ground state oxygen concentration can be depleted by the continuous excitation of the sample with the red laser, allowing some UC to occur.

Hence, we measure the response of the combined UC-SC system with the pump and probe beams aligned and misaligned, respectively. In the latter case the pump still irradiates the solar cell, to retain steady conditions in the SC, but without overlap with the probe beam on the UC unit. Since TTA-UC is a quadratic process at low irradiation, the linear response of the UC unit is zero for the small probe intensities used here.

Calculation of solar concentration

The sensitizer molecules harvest photons available for UC with their respective absorption Q-bands. We can calculate the excitation rate k_ϕ, brought about by 1⊙ in the UC unit, which is behind a SC with a transmission spectrum T_{SC}, from the absorption cross section σ in cm^2 and the photon flux density ρ in photons per cm^{-2} s^{-1} nm^{-1} of the AM1.5 standard solar spectrum by integrating over the respective porphyrin Q-band, $k_\phi = \int \rho(\lambda) T_{SC}(\lambda)\sigma(\lambda)d\lambda$. This yields $k_\phi = 2.1$ s^{-1} and $k_\phi = 1.9$ s^{-1} for PQ_4Pd (600–710 nm, 50 nm a-Si:H SC) and PQ_4PdNA (600–750 nm, 100 nm a-Si:H SC), respectively. The next step is to calculate the number of triplets brought about by the irradiation I^{pump} of the pump source in photons per area per time considering the irradiation of the UC unit through the SC, *i.e.* $k_\phi^{pump} = \sigma(670\text{nm}) * T_{SC}(670\text{nm}) * I^{pump}$. The ratio k_ϕ^{pump}/k_ϕ gives then the effective solar concentration.

Results

The external quantum efficiency (EQE), measured under short circuit conditions at room temperature, of two different bifacial a-Si:H *p-i-n* solar cells with *i* -layer thicknesses of 50 and 100 nm are plotted in Fig. 2 (a) and (b), respectively. The EQE curves drop considerably at the wavelengths coincident with the Q-band absorption maxima of the respective sensitizers, while the optical transmission of the bifacial cells approaches the maximum (about 40%). Further, the rubrene fluorescence spectrum (520–650 nm) was calculated to result in photon to electron conversion efficiencies of 21% and 43% for the 50 nm and 100 nm solar cell, respectively. Hence a-Si:H SCs are capable of utilizing the UC photons with reasonable efficiency.

The relative efficiency increase obtained from the comparison of the EQE measurement with pump and probe beam aligned and misaligned, respectively, are displayed by the symbols in Fig. 5. A SC with a 50 nm thick *i* -layer was combined with the PQ_4Pd-UC mixture (Fig. 5 (a)) and a 100 nm SC with the PQ_4PdNA-UC mixture (Fig. 5 (b)). The error bars represent standard deviations from point averaging at the respective wavelengths. The straight lines depict the expected enhancement profiles, which are calculated from the respective sensitizer absorption spectrum multiplied by the lamp spectrum (convolved with the spectral width of the monochromator) and the ratio of the solar cell transmission and EQE at each wavelength.

The peak enhancements of the solar cells were found to be (1.8 ± 1)% at 670 nm under (174 ± 12) ⊙ (equivalent to

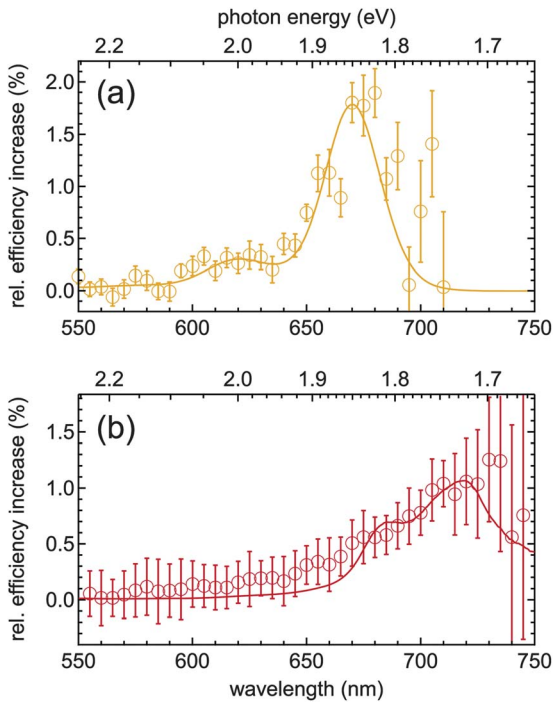

Fig. 5 Effect of UC unit on the solar cell performance from the ratio of SC response curves. (a) 50 nm a-Si:H solar cell and PQ_4Pd as TTA-UC sensitizer, (b) 100 nm a-Si:H solar cell and PQ_4PdNA. The error bars represent standard deviations from point averaging at each wavelength and are larger for (b) because of the lower probe intensity (factor 10). The straight lines display the expected spectral shape (see text).

676 mWcm^{-2} pump intensity) and (1.0 ± 0.2)% at 720 nm under (48 ± 3) ⊙ (471 mWcm^{-2}) for the two systems, respectively. We can calculate the total short circuit current density increase of the respective solar cells due to UC, under the equivalent solar concentrations as

$$\Delta J_{SC}^{UC} = e\int \Delta EQE^{UC}(\lambda) f_c \rho(\lambda) d\lambda, \quad (1)$$

where e is the elementary charge, f_c the concentration factor, $\rho(\lambda)$ is the AM1.5 solar flux in photons per area per time per wavelength, and $\Delta EQE^{UC}(\lambda)$ is the difference of the EQE measurements with pump and probe beams aligned and misaligned, respectively. Under the experimental conditions we obtain $\Delta J_{SC}^{UC} = 0.86$ mA cm^{-2} and $\Delta J_{SC}^{UC} = 0.30$ mA cm^{-2}, for the PQ_4Pd and PQ_4PdNA UC mixtures, respectively.

Discussion

While the peak EQE enhancements demonstrate proof-of-principle, the measured ΔJ_{SC}^{UC} values correspond to overall relative energy conversion efficiency increases of 0.10% and 0.07% for the two systems. Nevertheless, as explained below, despite the unoptimized nature of the current device, it is 200 times more effective than previously applied UC technologies which employ rare earth ions.

Comparison to rare-earths

Thus far, UC applied to SCs has been most commonly attempted with rare earth ions,[21] in particular the Yb^{3+}/Er^{3+} couple.[9,22] This UC mechanism is based on the spectrally narrow absorption band of Yb^{3+} at 980 nm and two energy transfer steps to subsequently populate an intermediate and a higher excited Er^{3+} state. The (Laporte forbidden) Er^{3+} emission transitions are observed at 522, 540 and 635 nm. Recently, de Wild *et al.* applied a rare-earth UC phosphor (β-$NaYF_4$:Yb^{3+} (18%), Er^{3+} (2%)) to a-Si:H solar cells.[23] The maximum increase in current density in this measurement was about $\Delta J_{SC}^{UC} = 0.41$ mA cm^{-2}.

However, for a meaningful comparison to our measurement, the solar concentration factor should be accounted for. From the product of the solar spectrum and the normalised absorption spectrum of the UC phosphor[24] we calculate an absorbed intensity of 3.8 mW cm^{-2} per sun for Yb^{3+}. With the excitation conditions employed in Ref. [23], a concentration factor of 790 ⊙ is obtained. Since both UC processes are quadratic at low excitation power densities, we are interested in the current change per sun squared, which we denote ζ. As such, we obtain ζ = 2.8 × 10^{-5} and 13 × 10^{-5} mA cm^{-2} ⊙$^{-2}$ for our PQ_4Pd and PQ_4PdNA UC mixtures respectively; and 0.066 × 10^{-5} mA cm^{-2} ⊙$^{-2}$ for the rare earth UC. Note that de Wild *et al.* used a a-Si:H solar cell with thicker *i* -layer (500 nm), which leads to a respective fourfold and twofold higher EQE in the range of the upconverted light in comparison to our SCs with 50 nm and 100 nm *i* -layers.

In terms of the normalised additional current generated, photochemical UC outperforms rare earth UC by two orders of magnitude. Indeed, rare earth ions lack the intermediate energy level which triplet states of organic molecules naturally afford, and so are at a disadvantage. However, at this point, no UC system based on organic dye sensitization can efficiently harvest photons below about 900 nm,[25] mainly due to the decrease in lifetime of the electronic states involved. Hence the two UC approaches may find complementarity in future work, in particular because of the difference in spectral range harvested.

Outlook

It is the eventual goal to deploy TTA-UC under one sun illumination, and as such, the reported ζ-values should be improved by a factor of 10^4. While daunting, this can be envisaged through a combination of device architecture and chemical optimization. A precondition of efficient TTA is that the efficiency of the elementary TTA step is not limited by spin-statistics. It had been argued that the TTA process should be limited to an efficiency of 1/9, being the probability that two triplets yield a singlet upon interacting. We have shown that this is not the case,[17,18] since the triplet (3/9) and quintet (5/9) encounter complexes need not quench the energy stored in the individual triplet molecules. This is the case for molecules where the second excited triplet state T_2 is higher in energy than twice the excitation energy of T_1, as in rubrene.[26] Indeed, this result has been confirmed independently in studies on organic light emitting diodes (OLED) with rubrene[27] as emissive material, where TTA-induced emission was found to significantly exceed the limit expected from a simple spin-statistical consideration.

TTA-UC at low excitation is generally limited by the TTA kinetics, where the first order decay of the emitter triplet is faster than the encounter with another triplet emitter.[19] Under steady-state conditions, the rate of triplet state creation is equal to the rate of removal,

$$k_\phi[S] = k_1[T] + k_2[T]^2, \quad (2)$$

where k_ϕ is the rate of sensitizer excitation, and k_1 and k_2 are respectively the first and second-order decay constants of emitter triplet states. The symbols [*S*] and [*T*] denote the sensitizer ground state concentration and the emitter triplet concentration respectively. The first order rate constant, k_1, takes account of reverse intersystem crossing (and any pseudo first-order processes), while the second-order rate constant, k_2, includes the various triplet–triplet annihilation channels. Since triplet energy transfer from sensitizers to emitters is rapid and complete, one need only track the creation and decay of excited states. The upconverted photons are generated by the second order process, which we desire to dominate the decay kinetics. As such, we require the triplet concentration to be as high as possible. Solving the above quadratic equation,

$$[T] = \frac{-k_1 + \sqrt{k_1^2 + 4k_\phi[S]k_2}}{2k_2} \approx \frac{k_\phi[S]}{k_1}, \quad (3)$$

for an inefficient upconvertor.

Now, for a given chemical system, the only parameters over which one has any control are k_ϕ and [*S*]. While k_ϕ can be increased trivially by concentrating sunlight, that is not an option for a practical device. Nevertheless, it may be increased by introducing a thinner upconversion layer with a rear reflector. In so doing there is both the benefit of absorbing incoming sunlight in a thinner layer, and reflecting additional upconverted light

into the solar cell. Moreover, if the rear reflector is a Lambertian scatterer, rather than a specular mirror, the effective pathlength is increased for wavelengths either side of the absorption peak.

A simulation of the effect of introducing a thinner upconversion layer with a Lambertian reflector is shown in Fig. 6. The vertical scale is the upconversion output of the device as compared to the current configuration, and the horizontal scale is the product of the UC layer thickness, d, and the maximum absorption coefficient of the sensitizer, $\alpha = \ln(10)\varepsilon[S]$, where ε is the molar decadic extinction coefficient. A threefold improvement of the device is predicted where the thickness of the UC layer corresponds to the decay length for photons at the absorption peak, that is $d\alpha = 1$. For a sensitizer concentration of 4×10^{-4} M, this corresponds to a 100 μm layer.

But, the biggest improvement will come from reengineering the UC unit at the molecular scale. The average distance between the sensitizers under the current conditions is 17 nm. If this can be reduced by a factor of 4–5, then the sensitizer and therefore triplet concentration will be increased hundredfold. This is not possible with the current porphyrins, since they aggregate and crystallize at concentrations higher than presently employed. However, it should be possible by incorporating the chromophores into a supramolecular assembly or macromolecule. The simulated result of this scenario is shown in Fig. 6. The peak is also found at $d\alpha = 1$, where this now corresponds to a 1 μm film, with a Lambertian back reflector. Note that a thinner UC layer reduces material cost for the UC: In such a layer the conceivably expensive Pd would amount to ~0.02 USD/m^2. The result demonstrates that, barring detrimental side-effects, this upconvertor should be 300 times brighter than the device reported presently.

In addition to the 300-fold enhancement outlined above, further improvements are possible: Rubrene has a rather low TTA rate constant of 1×10^8 M^{-1}s^{-1},[18,20] which is two orders of magnitude below the diffusion limit. Other species have been demonstrated to exhibit k_2 values more than an order of magnitude higher than that of rubrene,[28] leading to commensurately higher UC output. Other improvements to k_ϕ can be achieved by mixing sensitizer molecules to broaden the absorption range[29] or the use of plasmonics to spatially localize the excitation light[30] to create higher local triplet densities.

Indeed, many second generation PV devices suffer from the inability to harvest the red or near infrared spectrum, and thus will benefit from augmentation with a UC layer operable under one sun. Since it is optically coupled to the PV device, photochemical UC may be deployed behind, for instance, bulk heterojunction or dye-sensitised solar cells. The presently employed a-Si:H cell has a rather slow drop-off in EQE. However, organic solar cells such as bulk heterojunction or dye-sensitized solar cells generally exhibit a sharp cut-off, which would allow a greater portion of the solar irradiance to reach an optimized upconvertor.

The presented experimental design allows characterisation of the UC layer *in situ*, and thus determination of the additional current generated by the UC layer, ζ, which is the quantity of technological interest. Determination of this quantity will allow fair comparison of the various UC-assisted devices to be reported in the future.

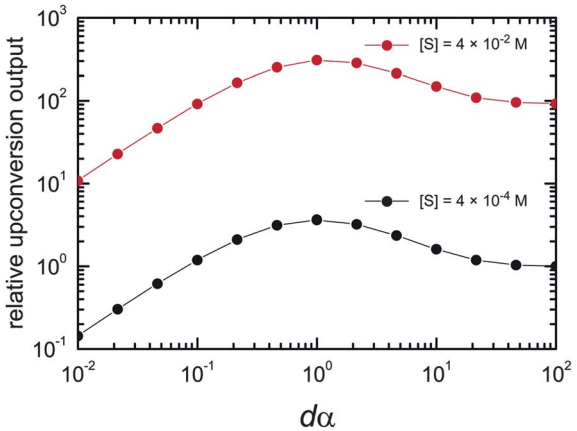

Fig. 6 Simulated upconversion performance as a function of UC layer thickness, d, for two sensitizer concentrations. A threefold enhancement is achieved with a Lambertian reflector and a thickness of $d = \alpha^{-1}$, where α is the peak absorption coefficient, $\alpha = \ln(10)\varepsilon[S]$. Increasing the sensitizer concentration one hundredfold yields a commensurate increase in UC performance.

Acknowledgements

Y.C. acknowledges The University of Sydney for a Henry, Bertie and Florence Mabel Gritton Scholarship. B.F. and T.F.S. acknowledge the Alexander von Humboldt-Foundation for respective Feodor Lynen fellowships. R.G.C.R.C. acknowledges the Australian Solar Institute for a postdoctoral research fellowship. K.L. is indebted to the Deutsche Forschungsgemeinschaft (DFG) for grant 583727 which initiated this German-Australian bilateral cooperation. We thank A. Stanco and Lastek for the gift of the 670 nm diode laser, M. Kaegi for making the SC holder, and T. Hänel (HZB) for EQE measurements. This research project is funded by the Australian Solar Institute, with contributions from The New South Wales Government and The University of Sydney. Aspects of this research was supported under Australian Research Councils Discovery Projects funding scheme (DP110103300). Equipment was purchased with support from the Australian Research Council (LE0668257). The work related to the SC preparation at HZB was funded by the Federal Ministry of Education and Research (BMBF) and the state government of Berlin (SENBWF) in the framework of the program "Spitzenforschung und Innovation in den Neuen Ländern" (03IS2151).

References

1 W. Shockley and H. J. Queisser, *J. Appl. Phys.*, 1961, **32**, 510.
2 M. A. Green, *Progr. Photovolt.: Res. Appl.*, 2009, **17**, 183.
3 M. A. Green, *Third Generation Photovoltaics: Advances Solar Energy Conversion* (Springer-Verlag, Heidelberg, 2003).
4 A. Shah, P. Torres, R. Tscharner, N. Wyrsch and H. Keppner, *Science*, 1999, **285**, 692.
5 L. C. Hirst and N. J. Ekins-Daukes, *Prog. Photovoltaics*, 2011, **19**, 286.
6 A. C. Atre and J. A. Dionne, *J. Appl. Phys.*, 2011, **110**, 034505.
7 A. Luque and A. Marti, *Phys. Rev. Lett.*, 1997, **78**, 5014.
8 N. J. Ekins-Daukes and T. W. Schmidt, *Appl. Phys. Lett.*, 2008, **93**, 063507.
9 J. de Wild, A. Meijerink, J. K. Rath, W. G. J. H. M. van Sark and R. E. I. Schropp, *Energy Environ. Sci.*, 2011, **4**, 4835.

10 T. Trupke, M. A. Green and P. Würfel, *J. Appl. Phys.*, 2002, **92**, 4117.
11 S. Baluschev, T. Miteva, V. Yakutkin, G. Nelles, A. Yasuda and G. Wegner, *Phys. Rev. Lett.*, 2006, **97**, 143903.
12 T. N. Singh-Rachford and F. N. Castellano, *Coord. Chem. Rev.*, 2010, **254**, 2560.
13 J. Z. Zhao, S. M. Ji and H. M. Guo, *RSC Adv.*, 2011, **1**, 937.
14 T. Miteva, V. Yakutkin, G. Nelles and S. Baluschev, *New J. Phys.*, 2008, **10**, 103002.
15 C. Wohnhaas, A. Turshatov, V. Mailander, S. Lorenz, S. Baluschev, T. Miteva and K. Landfester, *Macromol. Biosci.*, 2011, **11**, 772.
16 T. Khoury and M. J. Crossley, *Chem. Commun.*, 2007, 4851.
17 Y. Cheng, T. Khoury, R. G. C. R. Clady, M. J. Y. Tayebjee, N. J. Ekins-Daukes, M. J. Crossley and T. W. Schmidt, *Phys. Chem. Chem. Phys.*, 2010, **12**, 66.
18 Y. Cheng, B. Fückel, T. Khoury, R. G. C. R. Clady, M. J. Y. Tayebjee, N. J. Ekins-Daukes, M. J. Crossley and T. W. Schmidt, *J. Phys. Chem. Lett.*, 2010, **1**, 1795.
19 A. Monguzzi, J. Mezyk, F. Scotognella, R. Tubino and F. Meinardi, *Phys. Rev. B: Condens. Matter Mater. Phys.*, 2008, **78**, 5.
20 J. E. Auckett, Y. Cheng, T. Khoury, R. G. C. R. Clady, N. J. Ekins-Daukes, M. J. Crossley and T. W. Schmidt, *J. Phys.: Conf. Ser.*, 2009, **185**, 012002.
21 F. Auzel, *Chem. Rev.*, 2004, **104**, 139.
22 A. Shalav, B. S. Richards and M. A. Green, *Sol. Energy Mater. Sol. Cells*, 2007, **91**, 829.
23 J. de Wild, J. K. Rath, A. Meijerink, W. G. J. H. M. van Sark and R. E. I. Schropp, *Sol. Energy Mater. Sol. Cells*, 2010, **94**, 2395.
24 J. de Wild, A. Meijerink, J. K. Rath, W. G. J. H. M. van Sark and R. E. I. Schropp, *Sol. Energy Mater. Sol. Cells*, 2010, **94**, 1919.
25 B. Fückel, D. A. Roberts, Y. Cheng, R. G. C. R. Clady, R. B. Piper, N. J. Ekins-Daukes, M. J. Crossley and T. W. Schmidt, *J. Phys. Chem. Lett.*, 2011, **2**, 966.
26 F. Lewitzka and H. G. Löhmannsröben, *Z. Phys. Chem.*, 1986, **150**, 69.
27 D. Y. Kondakov, T. D. Pawlik, T. K. Hatwar and J. P. Spindler, *J. Appl. Phys.*, 2009, **106**, 124510.
28 T. N. Singh-Rachford and F. N. Castellano, *Inorg. Chem.*, 2009, **48**, 2541.
29 S. Baluschev, V. Yakutkin, G. Wegner, T. Miteva, G. Nelles, A. Yasuda, S. Chernov, S. Aleshchenkov and A. Cheprakov, *Appl. Phys. Lett.*, 2007, **90**, 181103.
30 S. Baluschev, F. Yu, T. Miteva, S. Ahl, A. Yasuda, G. Nelles, W. Knoll and G. Wegner, *Nano Lett.*, 2005, **5**, 2482.